Implementation of Firefly Algorithm in Optimal Sizing of Proton Exchange Membrane Fuel Cell - Battery Hybrid Locomotive

S. Ajayan*‡, A. Immanuel Selvakumar**

*Department of Electrical and Electronics Engineering, Karunya Institute of Technology and Sciences, Coimbatore, India.

** Department of Electrical and Electronics Engineering, Karunya Institute of Technology and Sciences, Coimbatore, India.

(ajayan85@gmail.com, immanuel@karunya.edu)

‡ S Ajayan; Tel: +91 8807870141, ajayan85@gmail.com

Received: 14.02.2020 Accepted:24.03.2020

Abstract- The intention of this work is to find out the sizes or ratings of fuel cell pack and battery which can meet the requirements of a medium-range passenger train with minimum cost. In this paper, two optimization techniques are used for component sizing of a passenger train with Proton exchange membrane (PEM) fuel cell and Battery. Proposed work deals with Indian Railways Palakkad-Nilambur passenger train. An objective function is formulated to reduce the cost of power sources, subject to various constraints such as battery SOC limits and PEM fuel cell rating, while considering the replacement costs of the power sources. Modeling of a locomotive, PEM fuel cell, the battery is done and evaluated/simulated for two driving cycles of the passenger train. Two energy management approaches are considered for the equilibrium of power from the two energy sources. Particle swarm optimization (PSO) and firefly algorithm (FA) are used to find the objective function solution and the results obtained in this way are discussed in detail. A number of extensive simulations validated that the heuristic FA studies provide a better environment in the field of component sizing with lower cost, small population size and early convergence than PSO.

Keywords: Energy management system, Firefly Algorithm, Component sizing, Particle Swarm Optimization, Hydrogen Fuel Cells, Electrical Vehicles.

1. Introduction

Environment pollution and global warming are the main topics of discussion by energy scientists all around the world. Scientists and researchers are therefore working towards clean, environmentally-friendly and economically viable renewable energy systems capable of replacing the rapidly depleting fossil fuels [1][2]. One such promising candidate is hydrogen [3]. Many vehicle manufacturers all around the world have come forward with huge investments for research and development of hydrogen-based renewable energy technology [4]. PEM fuel cell technology has attracted many researchers who are working with automobiles and locomotives, because of its higher efficiency, higher power density, and lower operating temperature. PEM fuel cells are very expensive and have a slow dynamic response, which hinders the candidate from replacing the traditional fossil fuel counterparts. In recent years, a lot of researchers are putting their heads together to overcome the technical difficulties of PEM fuel cell by adding energy storage devices like batteries or supercapacitors. This hybridization has shown good improvement in the dynamic response as well as hydrogen fuel consumption. Hence it is evident that, along with PEM fuel cell, some energy storage devices also have to be used which demands for an energy management system (EMS) [5]. Many researchers work with the energy management system with the objective of refining the PEM fuel cell system performance and reduce consumption of fuel. Researchers work with two approaches [6]: i) design optimization approach and ii) energy management optimization tactic as in Fig. 1.

The design optimization approach concentrates on optimal component sizing whereas the Energy management optimization approach deals with the development of energy-efficient and optimal energy management systems. Several topologies have been proposed by researchers using genetic algorithm (GA)[7], Dynamic programming (DP)[8], Bisection method, optimal control theory [9], fuzzy logic control (FLC)

[10][11], Adaptive search (AS) [12], rule-based deterministic algorithm [13], PSO [14][15], harmony search algorithm [16], [17] and so on. It can be perceived from literature that, research on fuel cell-based hybrid energy systems has been reported for both transportation and non-transportation applications [18]–[21].

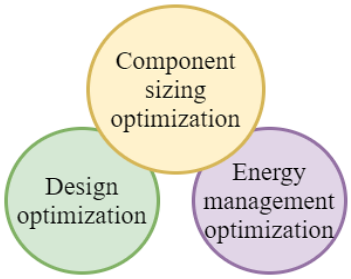

Fig. 1 Optimization Approaches

The present work basically concentrates on the transportation system and it can be seen from literature that only very few have worked on the effort of fuel cell hybrid energy system on locomotives. In [6], component sizing is carried out using PSO in which two energy management systems are considered and component ratings are optimized by taking care of degrading factors. In [22], FA grounded energy management system is projected for locomotive, in which consumption and fuel cost minimization are given key focus. However, component sizing optimization is not done. Many advanced metaheuristic algorithms can bring optimized solutions earlier than PSO and can converge to solution with a small population size, which is the motivation for this research work. Application of firefly algorithm (FA) for component sizing of the locomotive is unreported, to date. In India, diesel locomotives run in nearly 50% of the tracks because of a lack of electrification. And many of these tracks are through forest areas. The electrification of railway tracks in these areas will reduce the pollution, but it may indirectly increase the death of wild animals especially monkeys. In this paper, as a case study, a passenger train under Indian Railways (Palakkad-Nilambur) is considered which runs through thick green vegetation and forest areas of Nilambur. From the literature, following complications are identified: i) Need for a clean power source which is human and wild life friendly, ii) A good replacement for diesel engine which can provide a matching traction power, iii) An optimization problem to find the sizing of components for PEM fuel cell- Battery hybrid locomotive. A PEM fuel cell is a clean power source with zero emission and a PEM fuel cell-Battery hybrid system can be thought of in order to substitute the power demand of a diesel engine. The objective of this investigation is to develop an optimization tactic based on FA for component sizing of a hybrid battery-fuel cell system that can provide energy for an Indian locomotive.

The organization of the paper is as trails. Section 2 designates the modeling of various components of the hybrid source system. The generation of the objective function for the problem is dealt in Section 3. The proposed method is depicted in Section 4 and finally, the simulation results are debated under Section 5.

2. Modeling of the Hybrid Source System

The hybrid energy source system in this work contains PEM fuel cell as primary source of energy and battery as a secondary source of energy. The Lithium-ion battery pack is selected here as it has got many advantages such as lightweight, high density of power, high density of energy and longer lifetime [23]. The block diagram for a hybrid source system of a locomotive is as shown in Fig. 2.

This scheme work is planned to substitute the WDM-3A diesel engine [24] of the Palakkad-Nilambur passenger train. The same engine is used by Indian railways in many other routes as well. The passenger train under consideration has many intermediate stops between the source and destination. Also, it runs at various speeds which describes the driving cycle of the train. The demand for power varies rapidly and dynamically. During heavy acceleration, the battery packs supply the additional energy and during braking or deceleration, they absorb the regenerated energy. In this section, detailed modeling of the locomotive is described after which mathematical equations for PEM fuel cell and battery power also is described.

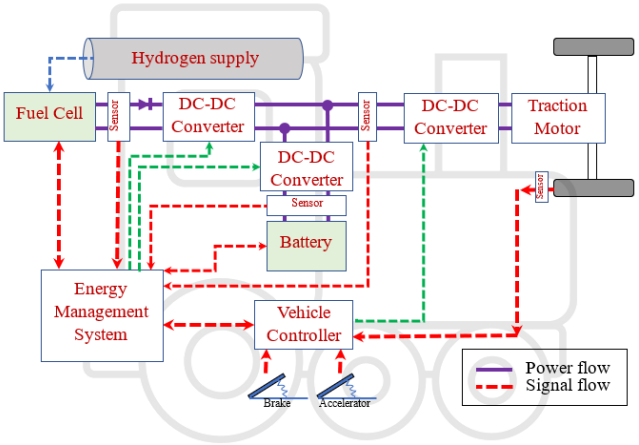

Fig. 2 Block diagram of FC locomotive

2.1 Model of locomotive

In this paper, a short to medium passenger train is considered. Modeling of such a locomotive is done to find the instantaneous power demand by mathematically formulating the various forces acting on the vehicle.

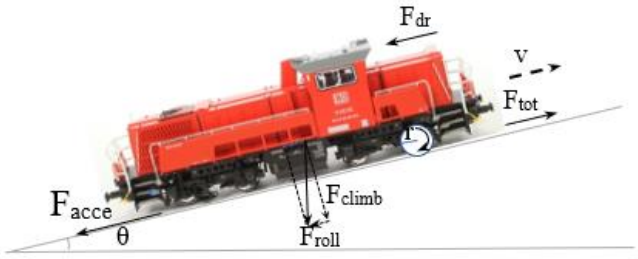

Fig. 3 Forces acting on a locomotive

The various forces include acceleration force, aerodynamic drag, the force of friction between the train wheels and the track and climbing force to overcome a slope as shown in Fig. 3 and are given by the following equations [25].

$$F_{acce}(t) = M_{loco}\, dv(t)/dt \quad (1)$$

$$F_{dr}(t) = 0.5\rho\ A\mu_d v(t)^2 \quad (2)$$

$$F_{roll}(t) = M_{loco} g \mu_r cos\theta \quad (3)$$

$$F_{clim}(t) = M_{loco} g sin\theta \quad (4)$$

Where M_{loco}=locomotive mass (kg), v= velocity(m/s), ρ=air density ($1.293kg/m^3$), A= area of cross-section (m^2), μ_d=coefficient of drag, g = gravitational constant ($9.8m/s^2$), μ_r=coefficient of rolling resistance and θ=slope.

The total traction force acting on the locomotive by the summation of the above forces [25].

$$F_{trtot}(t) = F_{acce}(t) + F_{dr}(t) + F_{roll}(t) + F_{clim}(t) \quad (5)$$

Then, the instantaneous power demand of the locomotive is determined as

$$P_{dem}(t) = F_{trtot}(t).v(t)/\eta_{tran} \quad (6)$$

Where η_{tran} is the efficiency of the gearbox and other mechanical systems and is presumed as 80% in this study. A small share of the power produced by the fuel cell will be used by fuel cell supporting equipment, cooling fans for traction motor and for lighting. Hence, total power demand is given by

$$P_{total}^{dem}(t) = P_{dem}(t) + P_{sup} \quad (7)$$

2.2 Model of PEM fuel cell

A typical Fuel Cell System is a power system that produces electrical power from a reaction between hydrogen and oxygen through a membrane [26]. Widely used technology for mobile applications is PEM fuel cell [27]. A schematic diagram of PEM fuel cell and the electrochemical reactions are as shown in Fig. 4. Water is the by-product of the reaction.

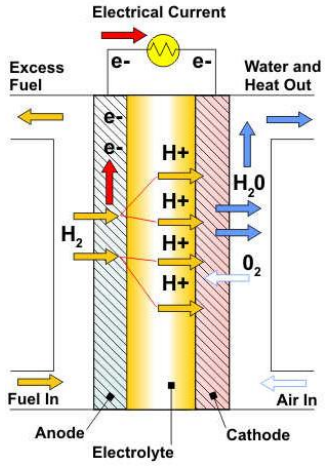

Fig. 4 Fuel cell

The cell potential of PEM fuel cell is given theoretically by the Nernst equation [28] as

$$E = E_0 - \frac{RT}{nF} ln\left(\frac{p_{H_2O}}{p_{H_2}(p_{O_2})^{0.5}}\right) \quad (8)$$

Where E_0 is the PEM fuel cell open-circuit voltage, value of R is $8.314J/mol$ (universal gas constant), T is the cell temperature, F is Faraday constant ($96{,}450C/mol$), n is the amount of electrons produced during electrochemical reaction, $p_{H_2O}$is the partial pressure of water, $p_{H_2}$and $p_{O_2}$are respectively the partial pressures of hydrogen and oxygen. E_0 is 1.229 V, if the state of chemical reaction exhaust product is in the liquid and 1.18 V if it is gaseous. All the voltages correspond to the temperature of 298.5K and p_{H_2} and $p_{O_2}$of 1 atm. Nevertheless, due to many losses occurring in the fuel cell, the actual cell voltage is lower than the theoretical value. Such losses often include activation loss, ohmic loss, and concentration loss. Thus, the actual cell voltage is given by [28].

$$v_{fc} = E - v_{act} - v_{ohm} - v_{conc} \quad (9)$$

A standard polarization graph showing the current density of the PEM fuel cell voltage, is as portrayed in Fig. 5.

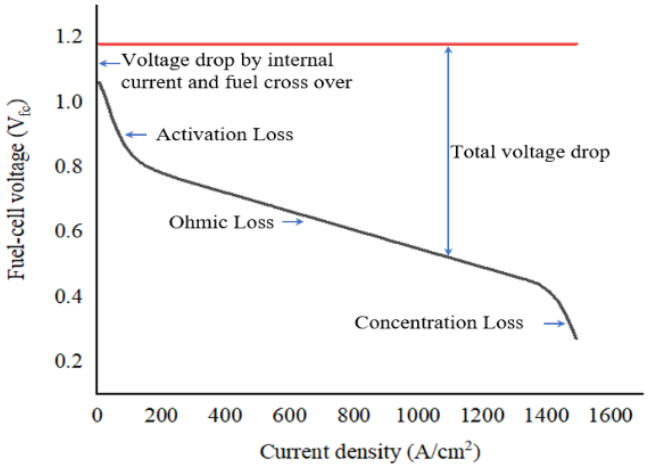

Fig. 5 Polarization curve

The efficiency of the PEM fuel cell stack (η_{fc}) is defined as the ratio of the produced electrical power (P_{fc}) to the hydrogen power (P_{H_2}). The theoretical efficiency is mathematically expressed as

$$\eta_{fc} = \frac{P_{fc}}{P_{H_2}} \quad (10)$$

Where,

$$P_{fc} = v_{fc} \times i_{fc} \quad (11)$$

$$P_{H_2} = mH_2 \times \Delta H \quad (12)$$

$$m_{H_2} = \frac{mi_{fc}}{nF} \quad (13)$$

$$\eta_{fc} = \frac{v_{fc} \times i_{fc}}{\frac{mi_{fc}}{nF}.\Delta H} = \frac{v_{fc}}{\frac{m}{nF}\Delta H} \quad (14)$$

Where P_{fc} is the PEM fuel cell power output, mH_2 is the rate at which hydrogen fuel is consumed, ΔH represents enthalpy, m is the molecular weight of hydrogen (2.016g) and n is the figure of electrons produced during the chemical reaction (n=2).

In [3], the efficiency of PEM fuel cell is factor that depends on the part-load ratio (PLR). The term PLR is defined as the ratio of PEM fuel cell electrical power to the rated power [21]. The mathematical equations to map PEM fuel cell efficiency are given by Eq. (15) and Eq. (16) and is shown in Fig. 6.

For $PLR(t) < 0.05$, $\eta_{fc}(PLR)$=0.27 (15)

For $PLR(t) \geq 0.05$, $\eta_{fc}(PLR) = 0.9033 \times PLR(t)^5 - 2.996 \times PLR(t)^4 + 3.6503 \times PLR(t)^3 - 2.0704 \times PLR(t)^2 + 0.4623PLR(t) + 0.3747;$ (16)

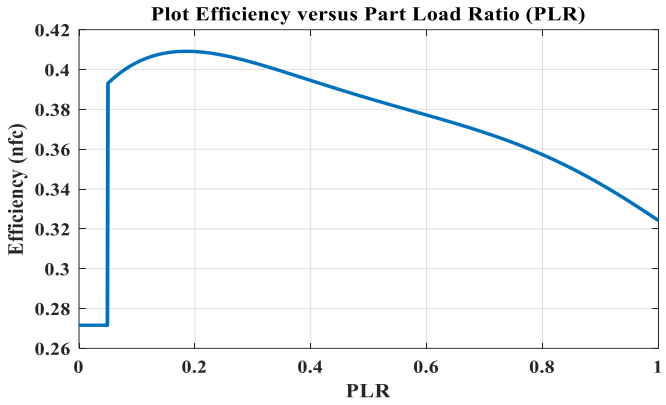

Fig. 6 Efficiency vs PLR

The fuel consumed by PEM fuel cell and heat generated during a particular driving period can be calculated from Eq. (10) to (12), as given by Eq. (17) and Eq. (18).

$$m_{H_2} = \int \frac{P_{fc}}{\Delta H.\eta_{fc}(PLR)} dt = \int \frac{P_{fc}}{LHV.\eta_{fc}(PLR)} dt \quad (17)$$

$$Q_{heat} = m_{H_2} \times \ LHV \quad (18)$$

where, $\eta_{fc}(PLR)$ is the efficiency of PEM fuel cell and LHV represents the lower heating value of hydrogen. However, it is important to note that the PEM fuel cell system has got some components such as valves for controlling the fuel. They cannot be opened or closed instantly, which results in slow dynamic response and hence limits the rate of power production. This slowing down is represented by ramp limit (R_{limit}).

$$R_{limit} = \frac{0.9\ P_{out}^{fc}}{30\ sec} \quad (19)$$

$$\frac{dP_{out}^{fc}}{dt} = \ R_{limit} \quad (20)$$

$$\int dP_{out}^{fc} = \int R_{limit}.dt \quad (21)$$

Hence, the instantaneous power output of PEM fuel cell $P_{out}^{fc}(t)$ is given by:

$$P_{out}^{fc}(t) = R_{limit}.t + P_{initial}^{fc} \quad (22)$$

Where $P_{initial}^{fc}$ is the initial output power of PEM fuel cell just before the acceleration or deceleration.

2.3 Model of Li-ion battery

Because of its many advantages, Lithium-ion battery is used in this analysis [29]. It acts as a buffer supplying additional power to the locomotive during heavy acceleration and receives power during regenerative braking. The power supplied by the battery is given by

$$P_{bat}(t) = P_{total}^{dem}(t) - P_{out}^{fc}(t) \quad (23)$$

$$SOC(t) = SOC(t - \delta t) - \eta_{bat}.\frac{P_{bat}(t)}{Q_{rated}^{bat}}.\delta t \quad (24)$$

Where η_{bat} is the efficiency of the battery, Q_{rated}^{bat} is the battery rated capacity and δt is a minor sample of time. For Lithium-ion battery, the charging and discharging efficiencies are 98% and 96% respectively [30],[31].

2.4 Locomotive driving cycles

In this paper, two driving cycles of Palakkad-Nilambur passenger train are considered. Driving cycles gives the data of vehicle velocity and its acceleration rate from which the vehicles' power demand can be calculated. The two driving cycles considered are as given in Fig. 7 and Fig. 8. The data is taken from [24], which are the actual data of the WDM-3A Palakkad-Nilambur passenger train.

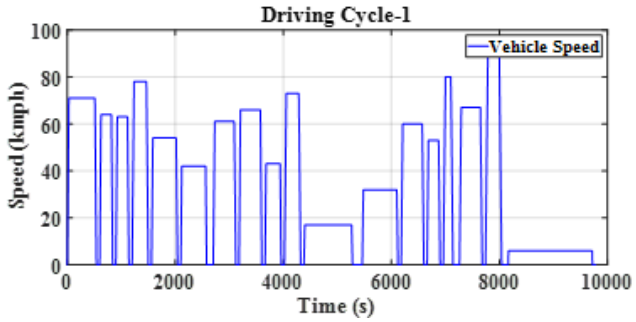

Fig. 7 Driving cycle -1

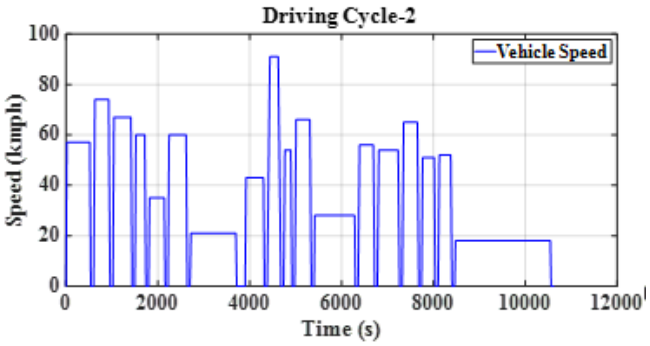

Fig. 8 Driving cycle 2

2.5 Energy management systems

The energy management system (EMS) is operated to determine the instant power drawn from the two sources as per the requirement of the locomotive. This paper considers two EMS proposed by Upasana and Ganguly [6]. The considerations for EMS-1 are as follows: When the locomotive is started, the generated power of fuel cell, P_{out}^{fc}

increases till it reaches the rated power, P_{rated}^{fc}. The rate of increase is limited by ramp limit constant. The generated power decreases during the deceleration of the vehicle constrained by the ramp limit constant. The battery is operated in charging or discharging or idle mode. If the instantaneous power demand is more than the PEM fuel cell generated output power, then battery discharges to supplement the shortage of power (battery power positive). If the instant power demand is lower than the PEM fuel cell generated output power, then the battery stores the extra generated power (battery power negative). And the considerations for EMS-2 are as follows: When the locomotive is started, the generated fuel cell power, P_{out}^{fc} increases till it reaches the rated power, P_{rated}^{fc} and operates at the rated power throughout the driving cycle. The PEM fuel cell generated power does not decrease or increase as per the dynamic changes in power demand but remains constant.

Pertaining to the instant power demand and generated fuel cell power, the battery operates in a similar way as in EMS-1, charging or discharging or idle mode. The working of two EMS is given in [6]. The computation time of the algorithm depends on the driving cycle chosen.

3. Formulation of Optimal Sizing Problem

The goal of this study is to find out the sizes or ratings of fuel cells and the battery which can meet the requirements of a medium-range passenger train with minimum cost. It is done with the help of cost minimization optimization. The objective function is expressed as:

$$f(x) = FC_{cost} + Batt_{cost} + Motor_{cost} + FC_{rep\_cost} + Batt_{rep\_cost} \quad (25)$$

Where, FC_{cost} is the cost of the PEM fuel cell system, $Batt_{cost}$ is the battery cost, $Motor_{cost}$ is the cost of traction motors, FC_{rep_cost}, $Batt_{rep\_cost}$ are costs of replacement of fuel cell and battery respectively. They are found out using the equations (26) to (30).

$$FC_{cost} = U_{fc}.P_{rated}^{fc} \quad (26)$$

$$Batt_{cost} = U_{Batt}.Q_{rated}^{bat} + const_{bat} \quad (27)$$

$$Motor_{cost} = U_{mot}.P_{rated}^{mot} + const_{mot} \quad (28)$$

$$FC_{rep\_cost} = \frac{FC_{fv}}{(1+i)^p}.FC_{rep} \quad (29)$$

$$Batt_{rep\_cost} = \frac{Bat_{fv}}{(1+i)^q}.Bat_{rep} \quad (30)$$

Where $U_{fc}, U_{Batt}, U_{mot}$ are per unit cost of fuel cell, battery and traction motor respectively; $const_{bat}$ and $const_{mot}$ are constant costs of battery and motor; FC_{fv} and Bat_{fv} are the future cost of fuel cell and battery; i is the rate of interest; p and q are the work-life of fuel cell and battery in years and FC_{rep} and Bat_{rep} are the number of replacements of fuel cell and battery for an estimated period. For this study, the values considered for the various parameters are as given in Table 1 [32].

The cost function (25) is a minimization optimization function with few constraints as follows:

$$SOC_{min} \leq SOC(t) \leq SOC_{max} \quad (31)$$

$$P_{total}^{dem}(t) = P_{bat}(t) \pm P_{out}^{fc}(t) \quad (32)$$

$$0 \leq P_{out}^{fc}(t) \leq P_{rated}^{fc} \quad (33)$$

$$P_{rated}^{fc} \geq P_{avg}^{dem} \quad (34)$$

Table 1 Parameters used in the problem

Parameter	Value	Parameter	Value
U_{fc}	47.67 $/kW	FC_{rep}	4
U_{Batt}	651.2 $/kWh	Bat_{rep}	1
U_{mot}	21.775 $/kW	i	0.07
$const_{bat}$	680 $	p	4 years
$const_{mot}$	425 $	q	10 years
		Estimated period	20 years

4. Component Sizing Optimization

4.1 Solution by Firefly Algorithm

Firefly algorithm (FA) is a metaheuristic optimization technique suggested by Xin-SheYang, inspired by fireflies' flashing light as shown in Fig. 9. FA showed better optimization efficiency when related with the particle swarm optimization (PSO) and genetic algorithm (GA). In FA, the fireflies are the solutions and the brightest firefly is the best solution [33][34]. Also, the attractiveness of the firefly depends on its brightness. All other fireflies get attracted to the brighter one. The attraction of each firefly is calculated as:

$$\beta = \beta_0.e^{-\gamma r^2} \quad (35)$$

where β_0 is the attraction at $r = 0$ and γ is the coefficient of light absorption.

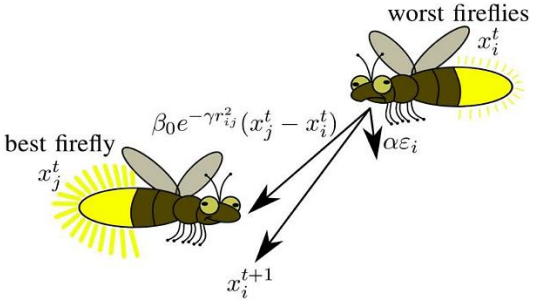

Fig. 9 Firefly Algorithm[35]

Suppose there are two fireflies i and j of which j is brighter, then the distance between any two fireflies i and j at x_i and x_j respectively, is $r_{ij} = x_i - x_j$. And i starts moving towards j and it updates its position as:

$$x_i = x_i + \beta_0.e^{-\gamma r_{ij}^2}(x_j - x_i) + \alpha\varepsilon_i \quad (36)$$

where the term $\alpha\varepsilon_i$ represents movement at random, α and ε_i are the parameter of randomization and random numbers vector respectively.

A design optimization tactic for locomotive application is proposed in this study and the detailed flow of operation is given in the flowchart as shown in Fig. 10.

A randomly generated population of fireflies is created initially after which brightness and cost object function of each firefly is calculated. Each of them is checked against the constraints and if not satisfied, a penalty is added based on the deviation from the constraint limit. Each firefly is a solution that gives optimized values of the sizing of PEM fuel cell and battery and is tested by calling EMS subroutine. All the fireflies now update the position as given by equation (36) and the process is repeated a number of times (Itr_{max}). The brightest firefly is chosen after a number of iterations and then simulated with the modeled equations. The simulation results are deliberated in the next section.

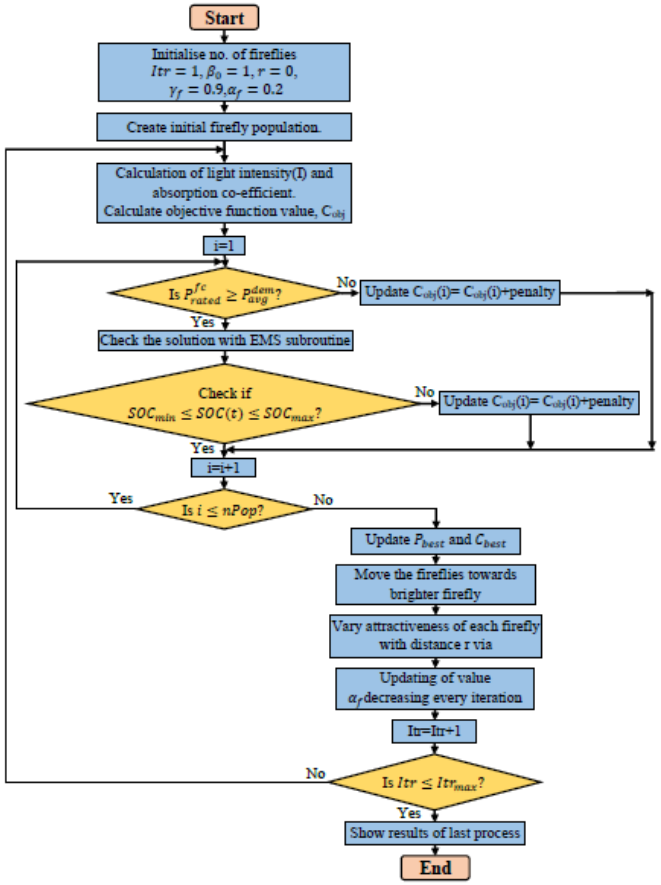

Fig. 10 Flowchart of FA

5. Results and Discussion

In this section, the simulation study results of FA are presented and compared with that of PSO algorithm. The objective of this work is to search optimal ratings of components of fuel cell driven locomotive. The SOC limits of battery are set to a minimum of 0.3 and a maximum of 0.9. The results are tabulated after running the algorithms over 20 sets of experimental iterations. The best results obtained are taken and used for discussion.

5.1. Sizing of PEM fuel cell and Lithium-ion battery

The optimal sizing of PEM fuel cell and Li-ion battery for the locomotive for driving cycle 1 and 2 are given in Table 2 and Table 3 respectively. It can be inferred that:

a) For both PSO and FA, the size of fuel cell is larger when Energy Management System 1 is selected.

b) It is noticed that, for both driving cycles, the P_{rated}^{fc} value is a little higher for FA heuristic method with a correspondingly lower Q_{rated}^{bat} value when compared with the PSO method. The minimized cost values are tabulated in Table 4 and discussed under section 4.4.

c) For a particular energy management system, the higher rating of components is chosen as the same locomotive covers both the driving cycles. For example, if energy management system 2 is chosen, a rating of 3.5594 MW and 2.4627 MWh is selected for PEM fuel cell and battery respectively.

Table 2 Values of PEM fuel cell and Battery ratings for Driving Cycle 1

Heuristic method	Energy Management Scheme			
	1		2	
	P_{rated}^{fc} (MW)	Q_{rated}^{bat} (MWh)	P_{rated}^{fc} (MW)	Q_{rated}^{bat} (MWh)
PSO	3.8642	2.1226	3.4020	1.8214
FA	3.8828	2.0536	3.4778	1.7043

Table 3 Values of PEM fuel cell and Battery ratings for Driving Cycle 2

Heuristic method	Energy Management Scheme			
	1		2	
	P_{rated}^{fc} (MW)	Q_{rated}^{bat} (MWh)	P_{rated}^{fc} (MW)	Q_{rated}^{bat} (MWh)
PSO	4.0816	2.7043	3.4687	2.6598
FA	4.1994	2.4865	3.5594	2.4627

5.2. Analysis of PSO dynamics of battery and PEM fuel cell

This section gives an analysis of the solution of PSO heuristic method for driving cycle 1 and 2. Fig. 11 and Fig. 12 shows the values of SOC and power demand respectively, for driving cycle 1 when the locomotive uses Energy Management System 1. The battery SOC lies inside the limits of 0.9 and 0.3, with the initial value being 0.8.

Similarly, Fig. 13 and Fig. 14 shows the instantaneous values of SOC and power for the locomotive for driving cycle 2 when Energy Management System 2 is used.

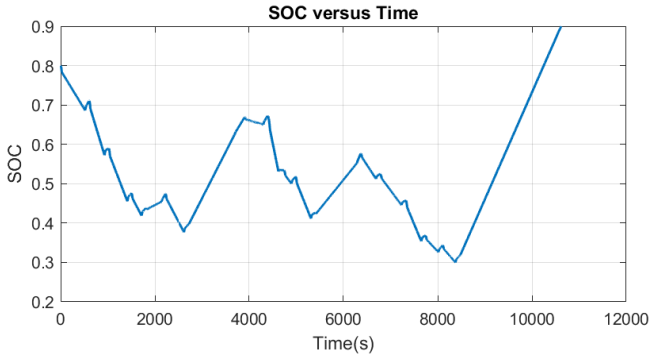

Fig. 11 Variation of SOC for EMS 1 and driving cycle 1 with PSO

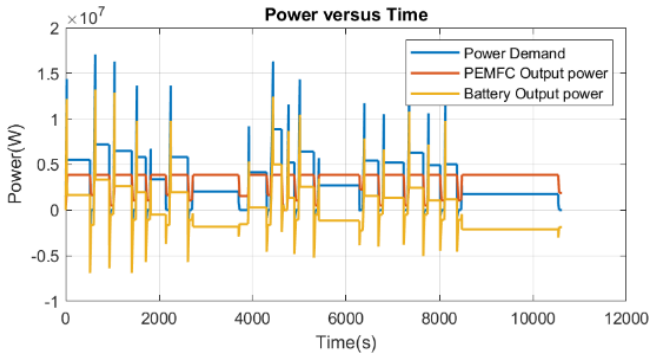

Fig. 12 Variation of various power for EMS 1 and driving cycle 1 with PSO

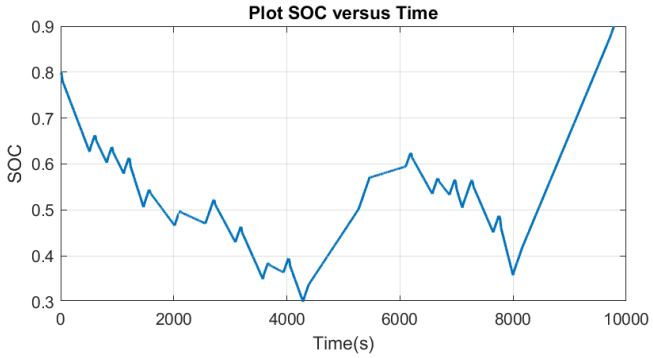

Fig. 13 Variation of various power for EMS 2 and driving cycle 2 with PSO

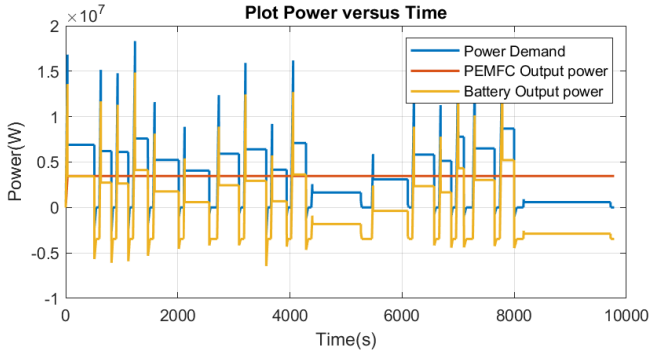

Fig. 14 Variation of various power for EMS 2 and driving cycle 2 with PSO

5.3. Analysis of FA dynamics of battery and PEM fuel cell

This section discusses the results obtained after optimized sizing through FA heuristic method. The results as shown in Fig. 15, Fig. 16, Fig. 17 and Fig. 18 are obtained after entering the optimized solution of FA in Energy Management System-1. It can be perceived that the generated power of PEM fuel cell increases and decreases as the power demand. Also, the battery SOC is maintained within the limits. Even though the computation time for FA is a little higher than PSO, the algorithm converges to an optimized solution with a smaller number of populations (Table 5).

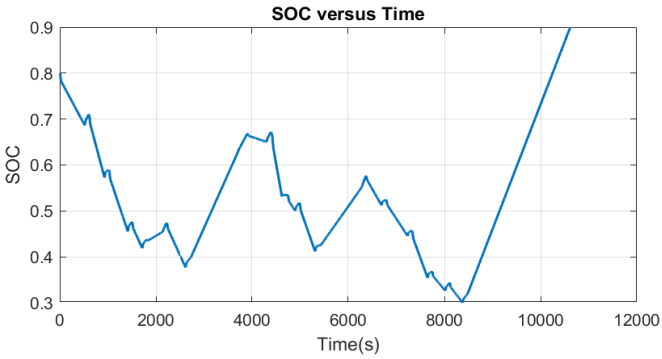

Fig. 15 Variation of SOC for EMS 1 and driving cycle 1 with FA

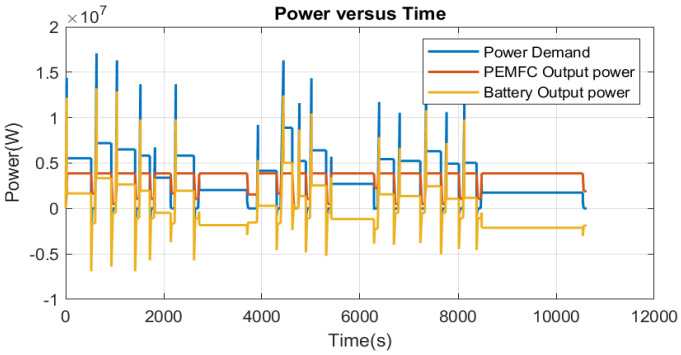

Fig. 16 Variation of various power for EMS 1 and driving cycle 1 with FA

The instantaneous values of SOC and power for driving cycle 1 are as shown in Fig. 15 and Fig. 16 respectively. Similarly, Fig. 17 and Fig. 18 gives the SOC and power, respectively, for driving cycle 2 with Energy Management System-1.

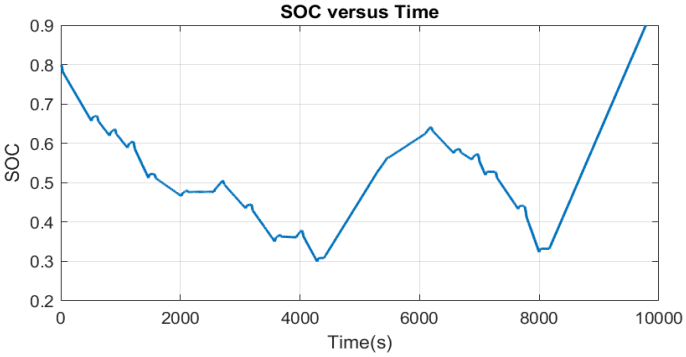

Fig. 17 Variation of various power for EMS 1 and driving cycle 2 with FA

The average locomotive power demand is subjected to the driving cycle.

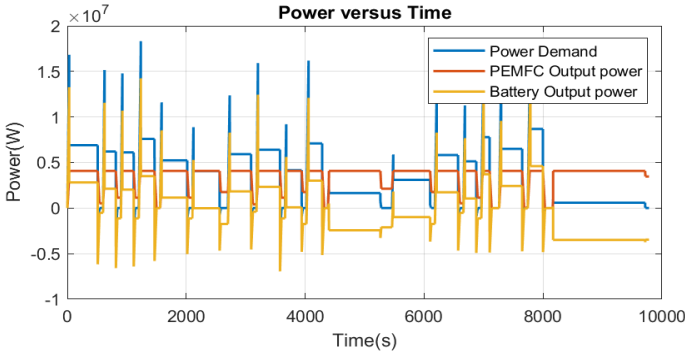

Fig. 18 Variation of various power for EMS 1 and driving cycle 2 with FA

In Energy Management System-2, the PEM fuel cell generated power equals the average power demand till the end of the driving cycle. Fig. 19 shows the SOC and Fig. 20 shows the power curves for driving cycle 1 with Energy Management System-2.

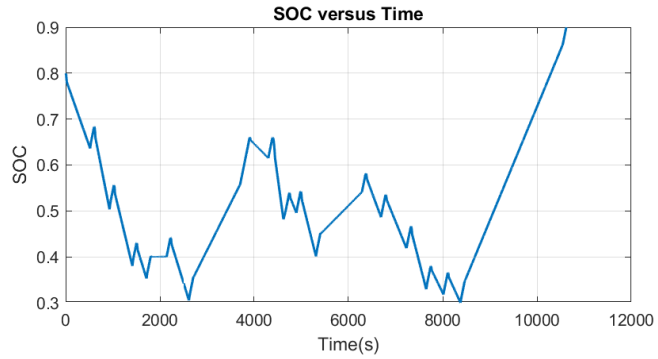

Fig. 19 Variation of various power for EMS 2 and driving cycle 1 with FA

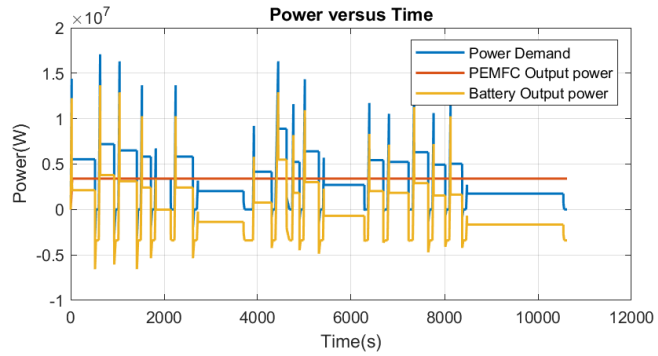

Fig. 20 Variation of various power for EMS 2 and driving cycle 1 with FA

Similarly, Fig. 21 and Fig. 22 gives the SOC and power curves for driving cycle 2 with Energy Management System-2. The negative power of battery indicates the charging state and positive the discharging state.

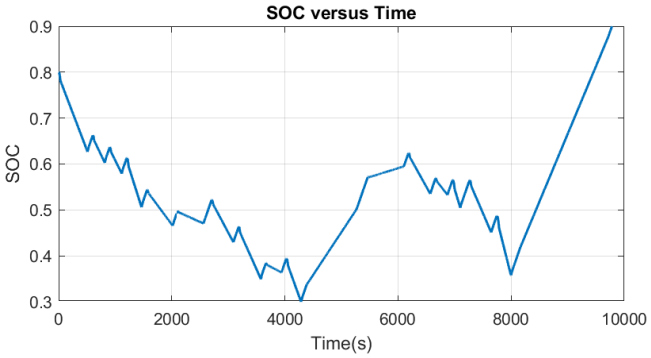

Fig. 21 Variation of various power for EMS 2 and driving cycle 2 with FA

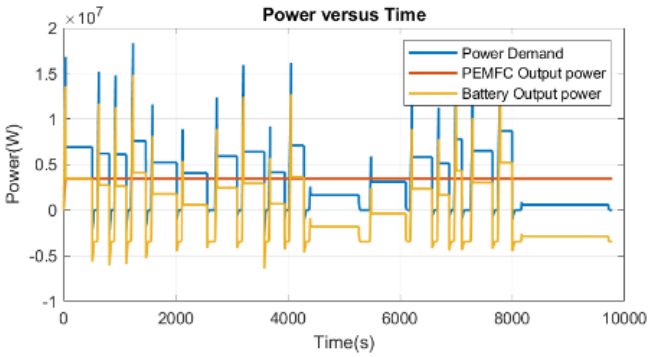

Fig. 22 Variation of various power for EMS 2 and driving cycle 2 with FA

5.4. Comparison between PSO and FA

The comparison of component sizing using two heuristic methods with two Energy Management Systems and two driving cycles are as depicted in Table 2 and Table 3.

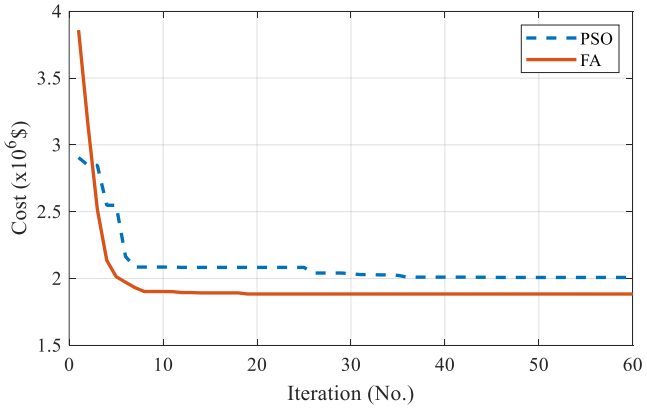

Fig. 23 Convergence behaviour of PSO and FA

Table 4 Total cost ($\times 10^6$ $)

Heuristic methods	Driving Cycle-1		Driving Cycle-2	
	Energy Management System-1	Energy Management System-2	Energy Management System-1	Energy Management System-2
PSO	1.6764	1.4582	2.0656	2.0074
FA	1.6324	1.3856	1.9294	1.8833

The performance analysis of PSO and FA is done on the basis of the cost function. The results are depicted in Fig. 23 and Table 4. The results show that the total cost is higher for the system with Energy Management System-1 for both PSO and FA for both the driving cycles. This is because of higher ratings of PEM fuel cell and battery capacity when Energy Management System-1 is used. Hence, as far as Energy Management Systems are considered, the Energy Management System-2 is less is having a low cost than the other. Referring to Fig. 23, FA converges to a solution at 19^{th} iteration (with a cost value of 1.8833 x 10^6\$) whereas PSO converges at 46^{th} iteration (with a cost value of 2.0074 x 10^6\$) for a test sample. The firefly algorithm method offers a better solution with lower cost function and early convergence to a solution when compared to PSO.

The system used for simulation is a Windows 10Pro 64-bit operating system with Intel Core i3-5005U CPU at 2 GHz with 12GB RAM. The computation time will be different for various systems and the number of parallel tasks executed. All the simulations were done on MATLAB platform. The details of simulations are as given in Table 5.

Table 5 Simulation details

Details		**PSO**	**FA**
No. of iterations per simulation		60	60
No. of population		200	25
Execution time			
Energy Management Scheme-1	Driving cycle 1	20m 30s	21m
	Driving cycle 2	20m 20s	19m 48s
Energy Management Scheme-2	Driving cycle 1	7m 15s	9m 30s
	Driving cycle 2	6m 42s	8m 48s

5.5. Fuel consumption comparison

The hydrogen consumed by the locomotive during the journey for both the driving cycles is determined and tabulated in Table 6. From the results, it is obvious that the locomotive fuel consumption is more when Energy Management System-2 is used as the PEM fuel cell continuously generates rated power from start till the end of the journey. Also, driving cycle 1 consumption is much higher than driving cycle 2 as the locomotive travels with a high-velocity profile in driving cycle 1. When compared with the results of PSO, the proposed FA method leads to a significant saving in the consumption of fuel for both the energy management systems and driving cycles. Engineers utilize the fuel consumption data for designing the hydrogen fuel tank capacity for the locomotives. Even though only the cost function for component sizing is included in the objective, this approach can be extended for optimal fuel consumption with different energy management systems and driving cycles.

Table 6 Total Fuel Consumption (kg)

Heuristic methods	Driving Cycle-1		Driving Cycle-2	
	Energy Management Scheme-1	Energy Management Scheme-2	Energy Management Scheme-1	Energy Management Scheme-2
PSO	878.8583	927.5097	837.7797	870.8103
FA	878.1774	912.1658	832.9415	866.1088

6. Conclusion

This paper investigates an idea for replacing the WDM3A diesel engine locomotive (DEL) with fuel cell-battery hybrid locomotive. A cost minimization objective function is framed incorporating the replacement cost of the hybrid sources considering an operation period of 20 years. The proposed PSO and FA methods are more influential and pertinent as compared to other metaheuristic methods which enhance the component ratings of the PEM fuel cell locomotive hybrid power system. The prescribed algorithms are established with two energy management systems as well as two driving cycles. The optimal sizes of the two power sources are obtained by running PSO and FA with energy management subroutine. The results clearly indicate that FA accomplished component ratings with a lower cost than PSO method. Also, the optimal sizes depend on the driving cycle, its average power demand and the energy management scheme used. A number of extensive simulations validated that the heuristic FA studies provide a better environment in the field of component sizing. FA substantializes that, it can offer a better optimal solution with lower cost, small population size and early convergence than PSO.

Future Scope

There is scope for adding another energy source such as solar panels or wind energy conversion systems and choosing optimal ratings for multiple sources. As the design optimization relies on energy management scheme, optimization-based energy management system subroutines with real time driving cycle data may give better results.

References

[1] A. Lahiani, A. Sinha, and M. Shahbaz, "Renewable energy consumption, income, CO_2 emissions, and oil prices in G7 countries: The importance of asymmetries," J. Energy Dev., vol. 43, no. 2, pp. 157–191, October 2018.

[2] F. Altun, S. A. Tekin, S. Gurel, and M. Cernat, "Design and Optimization of Electric Cars. A Review of Technological Advances," in 2019 8th International Conference on Renewable Energy Research and Applications (ICRERA), pp. 645–650, November 2019.

[3] J. Duan, Y. He, H. Zhu, G. Qin, and W. Wei, "Research progress on performance of fuel cell system utilized in vehicle," Int. J. Hydrogen Energy, vol. 44, no. 11, pp. 5530–5537, July 2018.

[4] G. Morrison, J. Stevens, and F. Joseck, "Relative economic competitiveness of light-duty battery electric and fuel cell electric vehicles," Transp. Res. Part C Emerg. Technol., vol. 87, pp. 183–196, January 2018.

[5] W. Yaici, L. Kouchachvili, E. Entchev, and M. Longo, "Dynamic Simulation of Battery/Supercapacitor Hybrid Energy Storage System for the Electric Vehicles," in 2019 8th International Conference on Renewable Energy Research and Applications (ICRERA), pp. 460–465, November 2019.

[6] U. Sarma and S. Ganguly, "Determination of the component sizing for the PEM fuel cell-battery hybrid energy system for locomotive application using particle

swarm optimization," J. Energy Storage, vol. 19, pp. 247–259, February 2018.

[7] S. F. Tie and C. W. Tan, "A review of energy sources and energy management system in electric vehicles," Renew. Sustain. Energy Rev., vol. 20, pp. 82–102, November 2013.

[8] S. Shojaabadi, S. Abapour, M. Abapour, and A. Nahavandi, "Simultaneous planning of plug-in hybrid electric vehicle charging stations and wind power generation in distribution networks considering uncertainties," Renewable Energy, vol. 99. Elsevier Ltd., pp. 237–252, 2016.

[9] Z. Yu, D. Zinger, and A. Bose, "An innovative optimal power allocation strategy for fuel cell, battery and supercapacitor hybrid electric vehicle," J. Power Sources, vol. 196, no. 4, pp. 2351–2359, 2011.

[10] D. Gao, Z. Jin, and Q. Lu, "Energy management strategy based on fuzzy logic for a fuel cell hybrid bus," J. Power Sources, vol. 185, no. 1, pp. 311–317, 2008.

[11] D. Zhou, A. Ravey, A. Al-Durra, and F. Gao, "A comparative study of extremum seeking methods applied to online energy management strategy of fuel cell hybrid electric vehicles," Energy Convers. Manag., vol. 151, pp. 778–790, October 2017.

[12] N. B. Arias, J. F. Franco, M. Lavorato, and R. Romero, "Metaheuristic optimization algorithms for the optimal coordination of plug-in electric vehicle charging in distribution systems with distributed generation," Electr. Power Syst. Res., vol. 142, pp. 351–361, May 2017.

[13] S. Njoya Motapon, L. A. Dessaint, and K. Al-Haddad, "A comparative study of energy management schemes for a fuel-cell hybrid emergency power system of more-electric aircraft," IEEE Trans. Ind. Electron., vol. 61, no. 3, pp. 1320–1334, 2014.

[14] I. Rahman, P. M. Vasant, B. S. M. Singh, and M. Abdullah-Al-Wadud, "On the performance of accelerated particle swarm optimization for charging plug-in hybrid electric vehicles," Alexandria Eng. J., vol. 55, no. 1, pp. 419–426, 2016.

[15] S. M. Hakimi and S. M. Moghaddas-Tafreshi, "Optimal sizing of a stand-alone hybrid power system via particle swarm optimization for Kahnouj area in south-east of Iran," Renew. Energy, vol. 34, no. 7, pp. 1855–1862, 2009.

[16] A. Maleki and F. Pourfayaz, "Sizing of stand-alone photovoltaic/wind/diesel system with battery and fuel cell storage devices by harmony search algorithm," J. Energy Storage, vol. 2, pp. 30–42, 2015.

[17] A. Maleki and A. Askarzadeh, "Comparative study of artificial intelligence techniques for sizing of a hydrogen-based stand-alone photovoltaic/wind hybrid system," Int. J. Hydrogen Energy, vol. 39, no. 19, pp. 9973–9984, 2014.

[18] M. Y. El-Sharkh, A. Rahman, and M. S. Alam, "Evolutionary programming-based methodology for economical output power from PEM fuel cell for micro-grid application," J. Power Sources, vol. 139, no. 1–2, pp. 165–169, 2005.

[19] A. Ghasemi, S. S. Mortazavi, and E. Mashhour, "Hourly demand response and battery energy storage for imbalance reduction of smart distribution company embedded with electric vehicles and wind farms," Renew. Energy, vol. 85, pp. 124–136, 2016.

[20] M. Y. El-Sharkh, M. Tanrioven, A. Rahman, and M. S. Alam, "Impact of hydrogen production on optimal economic operation of a grid-parallel PEM fuel cell power plant," J. Power Sources, vol. 153, no. 1, pp. 136–144, 2006.

[21] A. Maleki and M. A. Rosen, "Design of a cost-effective on-grid hybrid wind–hydrogen based CHP system using a modified heuristic approach," Int. J. Hydrogen Energy, vol. 42, no. 25, pp. 15973–15989, 2017.

[22] H. Zhang, J. Yang, J. Zhang, P. Song, and X. Xu, "A firefly algorithm optimization-based equivalent consumption minimization strategy for fuel cell hybrid light rail vehicle," Energies, vol. 12, no. 14, 2019.

[23] D. Yamashita, H. Nakao, Y. Yonezawa, Y. Nakashima, Y. Ota, K. Nishioka, M. Sugiyama "A new Solar to hydrogen conversion system with high efficiency and flexibility," 2017 6th Int. Conf. Renew. Energy Res. Appl. ICRERA 2017, vol. 2017-January, pp. 441–446, 2017.

[24] "India Rail Info: A Busy Junction for Travellers and Rail Enthusiasts." [Online]. Available: https://indiarailinfo.com/. [Accessed: 04-Feb-2020].

[25] M. Ehsani, Y. Gao, S. E. Gay, and A. Emadi, Modern electric, hybrid electric, and fuel cell vehicles: Fundamentals, theory, and design, Second Edition, CRC Press, pp.21-70, 2004.

[26] A. Rubio and W. Agila, "Dynamic Model of Proton Exchange Membrane Fuel Cells: A Critical Review and a Novel Model," in 2019 8th International Conference on Renewable Energy Research and Applications (ICRERA), pp. 353–358, 2019.

[27] W. Andari, A. Khadrawi, S. Ghozzi, H. Allagui, and A. Mami, "Energy Management Strategy of a Fuel Cell Electric Vehicle : Design and Implementation," Int. J. Renew. Energy Res., vol. 9, no. 3, pp. 1154–1164, 2019.

[28] F. Barbir, Pem Fuel Cells: Theory and Practice, Second Edition, Academic Press-Elsevier Ltd., 2012.

[29] F. Poloei, A. Bakhshai, and Y. F. Liu, "A novel online adaptive fast simple state of charge estimation for lithium ion batteries," 2017 6th Int. Conf. Renew. Energy Res. Appl. ICRERA 2017, vol. 2017-January, pp. 914–918, 2017.

[30] H. Fathabadi, "Combining a proton exchange membrane fuel cell (PEMFC) stack with a Li-ion battery to supply the power needs of a hybrid electric vehicle," Renew. Energy, vol. 130, pp. 714–724, June 2019.

[31] M. Belarbi, A. D. E. Kacher, and Z. Hallouz, "Operating limits of battery charge controllers," in 2019 8th International Conference on Renewable Energy Research and Applications (ICRERA), pp. 749–754, 2019.

[32] X. Wu, B. Cao, X. Li, J. Xu, and X. Ren, "Component sizing optimization of plug-in hybrid electric vehicles," Appl. Energy, vol. 88, no. 3, pp. 799–804, 2011.

[33] I. Fister, X. S. Yang, and J. Brest, "A comprehensive review of firefly algorithms," Swarm Evol. Comput., vol. 13, pp. 34–46, June 2013.

[34] X. S. Yang and X. He, "Firefly algorithm: recent advances and applications," Int. J. Swarm Intell., vol. 1,

no. 1, p. 36, 2013.
[35] E. Yoshimoto and M. V. T. Heckler, “Optimization of planar antenna arrays using the firefly algorithm,” J. Microwaves, Optoelectron. Electromagn. Appl., vol. 18, no. 1, pp. 126–140, 2019.